SCIENTIFIC REPORTS

OPEN

The M$_1$ muscarinic acetylcholine receptor subtype is important for retinal neuron survival in aging mice

Panagiotis Laspas[1], Mayagozel B. Zhutdieva[1], Christoph Brochhausen[2], Aytan Musayeva[1], Jenia Kouchek Zadeh[1], Norbert Pfeiffer[1], Ning Xia[3], Huige Li[3], Juergen Wess[4] & Adrian Gericke[1]

Muscarinic acetylcholine receptors have been implicated as potential neuroprotective targets for glaucoma. We tested the hypothesis that the lack of a single muscarinic receptor subtype leads to age-dependent neuron reduction in the retinal ganglion cell layer. Mice with targeted disruption of single muscarinic acetylcholine receptor subtype genes (M$_1$ to M$_5$) and wild-type controls were examined at two age categories, 5 and 15 months, respectively. We found no differences in intraocular pressure between individual mouse groups. Remarkably, in 15-month-old mice devoid of the M$_1$ receptor, neuron number in the retinal ganglion cell layer and axon number in the optic nerve were markedly reduced. Moreover, mRNA expression for the prooxidative enzyme, NOX2, was increased, while mRNA expression for the antioxidative enzymes, SOD1, GPx1 and HO-1, was reduced in aged M$_1$ receptor-deficient mice compared to age-matched wild-type mice. In line with these findings, the reactive oxygen species level was also elevated in the retinal ganglion cell layer of aged M$_1$ receptor-deficient mice. In conclusion, M$_1$ receptor deficiency results in retinal ganglion cell loss in aged mice via involvement of oxidative stress. Based on these findings, activation of M$_1$ receptor signaling may become therapeutically useful to promote retinal ganglion cell survival.

Glaucoma is a common neurodegenerative eye disease, which causes significant visual impairment at the terminal stage. It has been estimated that almost 80 million people worldwide will have glaucoma in 2020[1,2]. The disease is characterized by a progressive death of retinal ganglion cells (RGCs), specific anatomic alterations of the optic nerve and functional defects in the visual field[3].

Similar to other neurodegenerative diseases, deficits in natural cellular neuroprotective mechanisms may lead to a loss of neurons in the eye, especially under the presence of trigger factors like elevated intraocular pressure (IOP) and advanced age[4,5]. Cholinergic activation of the muscarinic acetylcholine receptor family, which is composed of five subtypes (M$_1$-M$_5$), exerts well-known neuroprotective effects in the brain[6]. Acetylcholinesterase inhibitors, which increase cholinergic activity, presently have clinical application in the management of Alzheimer's and Parkinson's disease[7,8]. However, their clinical utility is limited because of adverse effects associated with simultaneous activation of more than one muscarinic receptor subtype[9].

The neuroprotective properties of cholinergic stimulation in the brain are mostly attributed to M$_1$ receptor subtype activation. For that reason, new strategies are pursued in the therapy of Alzheimer's disease to selectively activate the M$_1$ receptor. Examples are the development of highly selective agonists for the M$_1$ receptor subtype[10] or the use of positive allosteric modulators, which selectively enhance M$_1$ receptor affinity to acetylcholine[11,12].

[1]Department of Ophthalmology, University Medical Center, Johannes Gutenberg University Mainz, Mainz, Germany. [2]Institute of Pathology, University Medical Center, Johannes Gutenberg University Mainz, Mainz, Germany. [3]Institute of Pharmacology, University Medical Center, Johannes Gutenberg University Mainz, Mainz, Germany. [4]Molecular Signaling Section, Laboratory of Bioorganic Chemistry, National Institute of Diabetes and Digestive and Kidney Diseases, National Institutes of Health, Bethesda, Maryland, USA. Correspondence and requests for materials should be addressed to P.L. (email: panagiotis.laspas@unimedizin-mainz.de)
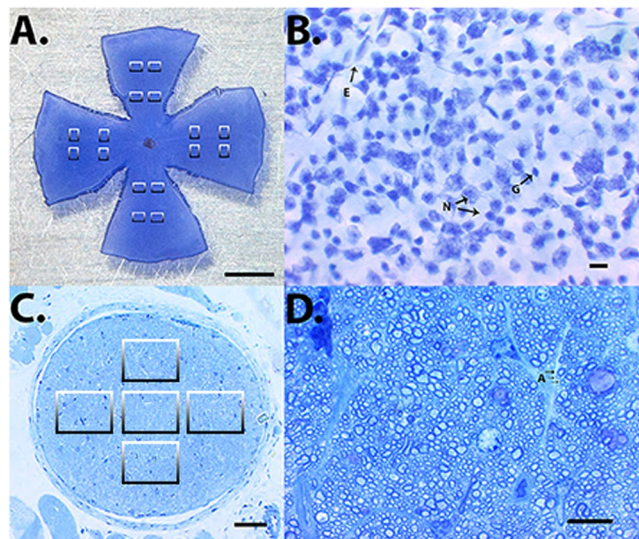
Figure 1. Photographs were taken from 16 pre-defined areas of wholemount stained with cresyl blue (**A**; scale bar 1 mm). In each photograph (**B**; scale bar 10 μm), the individual cell types were identified and separately counted (E: endothelial cell; G: glial cell; N: neuron). In optic nerve cross sections (**C**; scale bar 50 μm) the axon number (A: axon) was counted in 5 microphotographs taken from 5 pre-defined areas (**D**; scale bar 10 μm).

All five subtypes of the muscarinic receptor family have been identified in the eye, where they contribute to numerous physiological actions, such as regulation of IOP, pupil size, and ocular growth[13]. In the retina, muscarinic receptors are involved in modulating vasodilatation, cell-to-cell signaling and cell survival[14–16].

The goal of this study was to examine whether mutations affecting the expression of individual muscarinic receptor subtypes influence neuron survival in the retina. Our hypothesis was that the lack of a single muscarinic receptor subtype leads to age-dependent neuron reduction in the RGC layer. Because of the dearth of highly selective ligands for individual muscarinic receptor subtypes, we used N10 congenic mice of two different age categories, 5 and 15 months, respectively, each lacking one of the five muscarinic receptor subtypes for our studies.

Materials and Methods

Animals. All mice were treated in accordance with the EU Directive 2010/63/EU for animal experiments, and all experiments were approved by the Animal Care Committee of Rhineland-Palatinate, Germany. The generation of the different muscarinic receptor mouse knockout (KO) lines (M1R−/−, M2R−/−, M3R−/−, M4R−/−, and M5R−/−) has been described previously[17–21]. The genes that were knocked-out were Chrm1, Chrm2, Chrm3, Chrm4 and Chrm5, respectively. Each KO strain was backcrossed with C57BL/6NTac mice for 10 generations to obtain N10 congenic mice. Polymerase chain reaction (PCR) of DNA isolated from tail biopsies was used to identify the genotype of each animal. All KO mice are complete knockouts with no remaining receptor activity. Inbred C57BL/6NTac mice, throughout referred to as wild-type mice, served as controls.

Mice were housed under standardized conditions with a 12 h light/dark cycle, temperature of $22 \pm 2\,°C$, humidity of $55 \pm 10\%$, and with free access to food and tap water. Experiments were conducted in mice lacking a single muscarinic acetylcholine receptor subtype gene and in wild-type mice at the age of 5 and 15 months, respectively. Altogether there were 12 groups of 8 male mice.

Measurement of intraocular pressure. A TonoLab rebound tonometer (Bon Optic, Lübeck, Germany) was used for the measurement of IOP. This was conducted non-invasively in restrained conscious mice. Topical anesthesia with proparacaine 0.5% was used directly before each examination. Twelve IOP measurements were taken each time per eye, and the means for both eyes were calculated for each mouse. All measurements were conducted in the evening between 5.00 p.m. and 7.00 p.m.

Retinal wholemounts and cell counting. One randomly selected eye per mouse was obtained post mortem and fixed for one hour in 4% of paraformaldehyde (Sigma-Aldrich, Munich, Germany). Next, retinas were isolated in phosphate buffered solution (PBS, Invitrogen, Karlsruhe, Germany), and wholemounts were prepared, put on glass slides and stained with cresyl blue using a standard protocol as described previously[22]. A light microscope (Vanox-T, Olympus, Hamburg, Germany) connected to a Hitachi CCD camera (Hitachi, Düsseldorf, Germany) and equipped with Diskus software (Carl H. Hilgers, Königswinter, Germany) was used for the examination of wholemounts. Sixteen pre-defined areas per wholemount, eight central and eight peripheral, of 150 μm × 200 μm were photographed (Fig. 1A) by a blinded investigator. The proximal border of a central area was localized 0.75 mm from the center of the papilla. This distance corresponded to 5 heights of a photographed area. Each proximal border of a peripheral area was localized 0.75 mm from the distal border of a central photographed area. Thus, the distance from the center of the papilla and the proximal border of a peripheral area was 1.65 mm.

In each photograph (Fig. 1B) cells were counted manually by a blinded investigator using the cell counter plug-in for ImageJ software (NIH, http://rsb.info.nih.gov/ij/). After the photograph was opened in ImageJ under *plugins/analyze*, the *cell counter* tool was initialized. Using this, every cell was manually categorized and marked. Each marked cell was counted and assigned to the predefined category by the software. Cells were subdivided into three types based on morphological criteria of their nucleus (Fig. 1B). Neurons comprised presumptive RGCs with irregular outlines and a prominent nucleolus as well as presumptive displaced amacrine cells with a round or slightly oval, darkly staining nucleus of homogeneous size. Vascular endothelial cells were categorized based on long cell nuclei positioned along a blood vessel. Presumptive glial cells had a small darkly stained nucleus of variable shape. Next, from all 16 counted areas per retina, the average cell density was calculated. After measuring the surface of each wholemount with ImageJ and multiplying it with the cell density of each wholemount, the total number of cells per retina was calculated.

Optic nerve cross-sections and axon counting. Optic nerves were dissected, placed in fixative solution, postfixed and finally embedded in agar 100 resin. Later, semi-thin cross-sections were cut with an ultramicrotome (Ultracut E, Leica, Bensheim, Germany), placed on conventional glass slides and stained with 1% toluidine blue in 1% sodium borate according to standard protocols (Fig. 1C).

All cross-sections were examined through a light microscope (Vanox-T, Olympus) by a blinded investigator. In photographs of the whole cross-sections, we assessed their entire surface using ImageJ software. Five non-overlapping fields of $80\,\mu m \times 60\,\mu m$ (one central and four in the periphery) were photographed (Hitachi CCD camera) on every cross-section (Fig. 1C). The axons were counted manually on these photographs (Fig. 1D) using ImageJ software. After the photograph was opened in ImageJ under *plugins/analyze*, the *cell counter* tool was initialized. With this tool, each axon was manually marked and counted by the software. The mean axon density was calculated for all 5 counted areas per optic nerve cross section. The total number of axons per optic nerve was determined by multiplying the mean density by the cross sectional area, with was calculated with ImageJ.

Real-time PCR analysis. We used real-time PCR to determine the expression of different genes in the retina of aged wild-type and M1R−/− mice. Messenger RNA of prooxidative redox enzymes (nicotinamide adenine dinucleotide phosphate oxidases 1, 2, 4 - NOX1, NOX2, NOX4), of antioxidative redox enzymes (superoxide dismutase 1, 2, 3 - SOD1, SOD2, SOD3, glutathione peroxidase-1 - GPx1, heme oxygenese-1 - HO-1, catalase) and of intracellular regulatory proteins involved in aging (Sirtuin 1 - SIRT1, Sirtuin 6 - SIRT6, forkhead box protein O1 - FOXO1) was quantified.

After mice had been killed by CO_2 inhalation, the eyes were immediately removed and placed in ice-cold phosphate buffered solution (PBS, Invitrogen, Karlsruhe, Germany). The retina was isolated under a dissecting microscope by using fine-point tweezers and microscissors, then put into a 1.5-ml tube and immediately frozen in liquid nitrogen. Subsequently, tissue samples were homogenized (FastPrep; MP Biomedicals, Illkirch, France).

Gene expression was measured by SYBR Green based quantitative real time RT-PCR (qPCR), as previously described[23]. RNA was isolated using peqGOLD TriFast™ (PEQLAB) and cDNA was generated with the High Capacity cDNA Reverse Transcription Kit (Applied Biosystems, Darmstadt, Germany). Quantitative real time RT-PCR (qPCR) reactions were performed on a StepOnePlus™ Real-Time PCR System (Applied Biosystems) using SYBR® Green JumpStart™ Taq ReadyMix™ (Sigma-Aldrich, Munich, Germany) and 20 ng cDNA. Relative mRNA levels of target genes were quantified using comparative threshold (CT) normalized to housekeeping gene TATA-binding protein (TBP). The qPCR primer sequences are shown in Table 1.

DHE Staining. The oxidative fluorescent dye, dihydroethidium (DHE), dihydroethidium (DHE) was utilized to determine reactive oxygen species ROS levels *in situ* as described previously[24]. After mice had been sacrificed and their eyes harvested, $10\,\mu m$ frozen cross-sections were prepared. After thawing, the tissue sections were immediately incubated with 1 μmol/l dihydroethidium. Dihydroethidium is cell permeable and reacts with superoxide to form ethidium, which in turn intercalates in the deoxyribo nucleic acid, thereby exhibiting a red fluorescence. Photographs of retinal cross-sections were taken using a fluorescent microscope at an excitation wavelength of 520 nm and an emission wavelength of 610 nm. The intensity of the staining was measured in individual cell layers of the retina by using ImageJ software (NIH, http://rsb.info.nih.gov/ij/).

Statistical analysis. Data are presented as mean ± SD unless other stated, and n represents the number of mice (eyes) per group. For comparison of IOP, cell and axon number between young and old mice of the same genetic background, an unpaired t test was used. Different genotypes of the same age category were compared by one-way ANOVA and a Tukey's post hoc test. Messenger RNA expression levels (ΔCT values) were compared using an unpaired t test and are presented as relative units to wild-type controls. DHE staining intensity was compared using the Mann-Whitney U test and presented as box plots as relative units to wild-type controls. A value of $P < 0.05$ was defined as significant.

Results

Intraocular pressure. No significant differences in IOP were found between young and old mice of the same genetic background well as between individual mouse genotypes of the same age category (Fig. 2). The mean IOP in individual mouse groups was (5 versus 15 months): Wild-type 12.53 ± 2.479 versus 13.36 ± 1.914, p = 0.46; M1R−/− 12.77 ± 1.536 versus 13.45 ± 1.679, p = 0.41; M2R−/− 13.23 ± 1.924 versus 13.18 ± 1.464, p = 0.96; M3R−/− 11.96 ± 1.712 versus 12.37 ± 1.546, p = 0.62; M4R−/− 11.86 ± 1.774 versus 13.05 ± 2.087, p = 0.24; M5R−/− 12.11 ± 1.938 versus 12.92 ± 2.139, p = 0.44.

Number of cells in the RGC layer. The total number of cells in the RGC layer did not differ between young and old mice of all genotypes except M1R−/− mice, where the cell number was markedly reduced in aged mice (Fig. 3E).

TBP forward	CTT CGT GCA AGA AAT GCT GAA T
TBP reverse	CAG TTG TCC GTG GCT CTC TTA TT
NOX1 forward	GGA GGA ATT AGG CAA AAT GGA TT
NOX1 reverse	GCT GCA TGA CCA GCA ATG TT
NOX2 forward	CCA ACT GGG ATA ACG AGT TCA
NOX2 reverse	GAG AGT TTC AGC CAA GGC TTC
NOX4 forward	TGT AAC AGA GGG AAA ACA GTT GGA
NOX4 reverse	GTT CCG GTT ACT CAA ACT ATG AAG AGT
SOD1 forward	CCA GTG CAG GAC CTC ATT TTA AT
SOD1 reverse	TCT CCA ACA TGC CTC TCT TCA TC
SOD2 forward	GCT CTG GCC AAG GGA GAT G
SOD2 reverse	TGT CCC CCA CCA TTG AAC TT
SOD3 forward	TTC TTG TTC TAC GGC TTG CTA CTG
SOD3 reverse	AGC TGG ACT CCC CTG GAT TT
GPx1 forward	CCT TGC CAA CAC CCA GTG A
GPx1 reverse	CCG GAG ACC AAA TGA TGT ACT TG
HO-1 forward	GGT GAT GCT GAC AGA GGA ACA C
HO-1 reverse	TAG CAG GCC TCT GAC GAA GTG
Catalase forward	CAA GTA CAA CGC TGA GAA GCC TAA G
Catalase reverse	CCC TTC GCA GCC ATG TG
SIRT1 forward	GCC AAA CTT TGT TGT AAC CCT GTA
SIRT1 reverse	TGG TGG CAA CTC TGA TAA ATG AA
SIRT6 forward	TGG CCC CCA AGT TTG ACA
SIRT6 reverse	GCT GAA CCA GGG CCA TGT
FOXO1 forward	GCG GGC TGG AAG AAT TCA A
FOXO1 reverse	TTC CTT CAT TCT GCA CTC GAA TAA

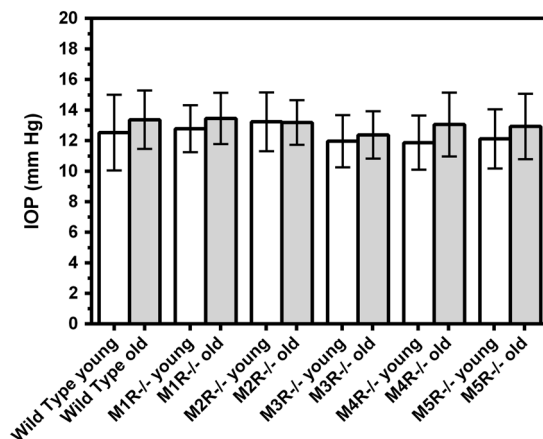**Table 1.** Primer sequences for qPCR of the genes examined in aged wild-type and M1R−/− mice.

Figure 2. Intraocular pressure (IOP) did not differ between young (5 months) and old (15 months) mice in any of the mouse groups. Also, no differences in IOP were seen between individual mouse genotypes of the same age category. Data are presented as mean ± SD (n = 8 per age category and genotype).

The total cell number in the individual mouse groups was (5 versus 15 months): Wild-type 113598 ± 9543 versus 109390 ± 15565, p = 0.53; M1R−/− 115981 ± 8897 versus 90625 ± 11414, ***p = 0.0002; M2R−/− 118012 ± 10529 versus 110575 ± 6623, p = 0.11; M3R−/− 115438 ± 8833 versus 110539 ± 14156, p = 0.42; M4R−/− 117008 ± 12050 versus 114250 ± 10086, p = 0.63; M5R−/− 122780 ± 11083 versus 112.747 ± 13697, p = 0.13. The total cell number in the RGC layer was also reduced in 15 month-old M1R−/− mice compared to all other genotypes of the same age category (*p < 0.05).

Looking at the subpopulations of cells, we found that 15-month-old M1R−/− mice had a markedly reduced number of neurons in the RGC layer compared to 5-month-old M1R−/− mice (Fig. 3F). In contrast, there were no age-dependent differences in neuron number between old and young mice of the other genotypes. The number of neurons in the individual mouse groups was (5 versus 15 months): Wild-type 101613 ± 10981 versus 97549 ± 14117, p = 0.53; M1R−/− 103362 ± 8438 versus 79028 ± 10752, ***p = 0.0002;

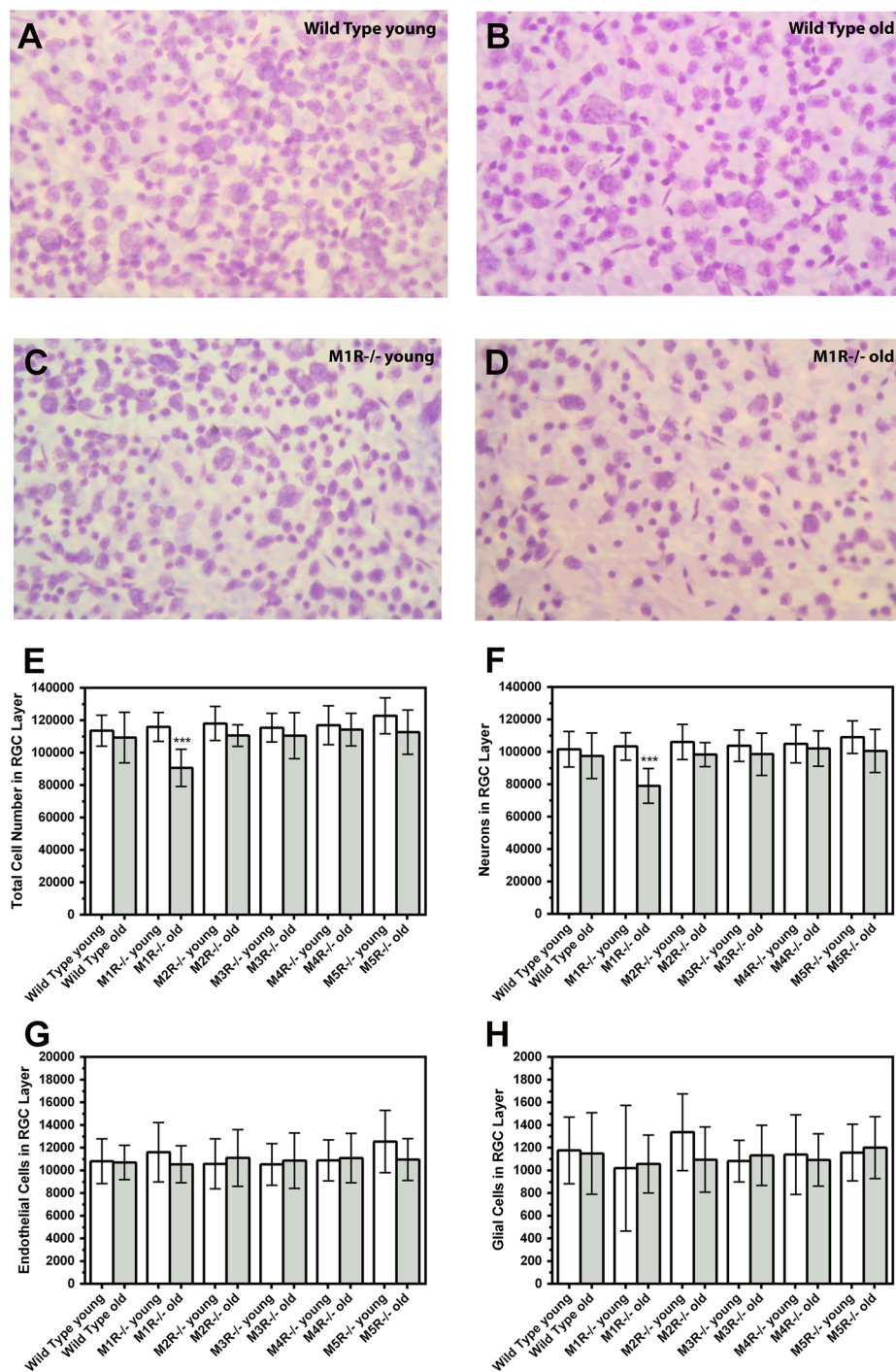## Cells in the Retinal Ganglion Cell Layer

Figure 3. Example photographs taken from retina wholemounts of wild-type and M1R−/− mice at both age categories (**A–D**; scale bars 10 μm). Total number of cells (**E**), of neurons (**F**), endothelial cells (**G**) and glia cells (**H**) in the RGC layer. The total number of cells and number of neurons in the RGC layer was found lower in old M1R−/− mice than in young mice of the same genetic background (***P < 0.001).

M2R−/− 106103 ± 10793 versus 98382 ± 7456, p $= 0.12$; M3R−/− 103833 ± 9660 versus 98552 ± 13045, p $= 0.37$; M4R−/− 104981 ± 11715 versus 102071 ± 10941, p $= 0.62$; M5R−/− 109084 ± 10021 versus 100592 ± 13310, p $= 0.17$. Neuron number in the RGC layer was also reduced in 15 month-old M1R−/− mice compared to all other genotypes of the same age category (*p < 0.05).

The subpopulation of endothelial cells localized in the RGC layer did not differ in any of the mouse genotypes (Fig. 3G). The number of endothelial cells in the individual mouse groups was (5 versus 15 months): Wild-type

10809 ± 1971 versus 10692 ± 1516, $p = 0.90$; M1R$-/-$ 11600 ± 2619 versus 10541 ± 1623, $p = 0.35$; M2R$-/-$ 10573 ± 2198 versus 11098 ± 2501, $p = 0.66$; M3R$-/-$ 10523 ± 1831 versus 10855 ± 2445, $p = 0.76$; M4R$-/-$ 10888 ± 1804 versus 11087 ± 2175, $p = 0.84$; M5R$-/-$ 12539 ± 2753 versus 10954 ± 1853, $p = 0.20$.

Also, the subpopulation of glial cells localized in the RGC layer did not differ in any of the mouse genotypes (Fig. 3H). The number of glial cells in the individual mouse groups was (5 versus 15 months): Wild-type 1176 ± 293 versus 1149 ± 359, $p = 0.87$; M1R$-/-$ 1019 ± 554 versus 1056 ± 256, $p = 0.87$; M2R$-/-$ 1337 ± 339 versus 1095 ± 288, $p = 0.15$; M3R$-/-$ 1082 ± 183 versus 1133 ± 265, $p = 0.67$; M4R$-/-$ 1140 ± 352 versus 1092 ± 230, $p = 0.75$; M5R$-/-$ 1157 ± 250 versus 1201 ± 273; $p = 0.74$.

Number of axons in optic nerve cross-sections. The number of axons in the optic nerve, which represent the number of RGC, was markedly reduced in 15-month-old compared to 5-month-old M1R$-/-$ mice (Fig. 4E). In contrast, no differences in axon number were found between young and old mice of all other genotypes. The whole axon number in individual mouse groups was (5 versus 15 months): Wild-type 55702 ± 5429 and 54721 ± 6269, $p = 0.74$; M1R$-/-$ 58455 ± 6252 versus 44210 ± 8069, **$p = 0.0015$; M2R$-/-$ 55585 ± 8346 versus 57636 ± 5362, $p = 0.57$; M3R$-/-$ 53789 ± 7359 versus 54443 ± 6838, $p = 0.86$; M4R$-/-$ 54131 ± 5562 and 53871 ± 6423, $p = 0.93$; M5R$-/-$ 58457 ± 6579 versus 54659 ± 8236, $p = 0.33$. The axon number in the optic nerve was also reduced in 15 month-old M1R$-/-$ mice compared to wild-type, M2R$-/-$ and M5R$-/-$ mice of the same age category (*$p < 0.05$).

Messenger RNA expression. Expression of the genes examined is presented in Fig. 5. Among the three prooxidative NOX isoforms (NOX1, NOX2, NOX4) that have previously been shown to be modified in different pathological conditions of the retina, NOX2 was found to be higher expressed in the retina of aged M1R$-/-$ mice compared to wild-type mice (*$p = 0.0157$). Interestingly, several antioxidative redox genes, including SOD1 (**$p = 0.0011$), GPx1 (*$p = 0.0324$) and HO-1 (****$p < 0.0001$), displayed lower mRNA expression levels in M1R$-/-$ mice than in wild-type mice. The expression levels of genes coding for intracellular regulatory proteins involved in aging, SIRT1, SIRT6 and FOXO1, did not differ between aged wild-type and M1R$-/-$ mice.

ROS levels in the retina. The DHE staining intensity was markedly higher in the RGC layer of aged M1R$-/-$ mice compared to age-matched wild-type mice (*$p = 0.0148$; Fig. 6A), indicative of increased ROS levels. In contrast, no significant differences in staining intensity between the two mouse genotypes were found in the inner nuclear layer (Fig. 6B) and the outer nuclear layer (Fig. 6C).

Discussion

There are two major new findings in the present study. First, the lack of the M$_1$ receptor age-dependently reduced survival of neurons in the RGC layer and of optic nerve axons, which represent the axons of RGC. Because the IOP was not affected by the lack of any of the five muscarinic receptor subtypes at any age, it is unlikely that IOP contributed to the neuron loss of aged M1R$-/-$ mice. Second, mRNA expression for the prooxidative redox enzyme, NOX2, was increased in aged M1R$-/-$ mice while mRNA expression for the antioxidative redox enzymes, SOD1, GPx1 and HO-1, was reduced. Moreover, the ROS level was increased in the RGC layer of aged M1R$-/-$ mice compared to wild-type of the same age, indicating that aged M1R$-/-$ mice had a reduced antioxidative capacity. This is the first study based on gene targeting technology supporting the concept that the neuroprotective effect of the cholinergic system in the RGC layer is mediated by the M$_1$ muscarinic receptor subtype.

Previous studies suggested that cholinergic muscarinic receptor activation exerts neuroprotective effects in retinal neurons. For example, activation of muscarinic receptors by carbachol, an acetylcholine analogue, promoted cell survival in rat RGC cultures. This effect was diminished by telenzepine, a M$_1$-preferring muscarinic receptor blocker, suggesting that the M$_1$ receptor might have mediated the neuroprotective effect observed previously[25]. Pilocarpine, a well-known muscarinic receptor agonist, was found to act protective against glutamate-induced apoptosis in rat retinal cell cultures. This effect was also attributed to the M$_1$ receptor, since it was blocked by pirenzepine, a M$_1$ receptor-preferring antagonist[26]. Moreover, in an *in vivo* study, the acetylcholinesterase inhibitor, galantamine, exerted neuroprotective actions in the rat retina, which were blocked by M$_1$-preferring muscarinic receptor antagonists[27]. In all these studies, the neuroprotective effect induced by cholinergic activation was reversed by pharmacological blockade of the M$_1$ receptor, suggesting its neuroprotective action. However, the selectivity of muscarinic receptor agonists and antagonists utilized in the above cited studies is limited, since the receptor subtypes have only minor differences in their orthosteric binding sites[28]. For example, pirenzepine has only a ten-fold higher affinity to the M$_1$ receptor than to all other muscarinic receptor subtypes[29]. Telenzepine shows a similar affinity profile[30]. Thus, a possible neuroprotective effect mediated via other muscarinic receptor subtypes cannot be excluded when using classical pharmacological ligands.

In order to circumvent this problem, we used mice with targeted disruption of single muscarinic receptor subtype genes (M$_1$–M$_5$) in the present study. We hypothesized, that if a specific muscarinic receptor subtype was responsible for the neuroprotective cholinergic effects in the retina, its total absence in gene-targeted mice would make neurons more prone to cell death.

In a previous study from our laboratory conducted on 5 month-old M1R$-/-$ mice of a mixed genetic background, we found that neuron number in the RGC layer and optic nerve axon number were not affected by M$_1$ receptor deficiency[31]. One possible explanation for these findings was that the M1R$-/-$ mice used in the previous study might have been too young to develop neuronal loss. Another explanation was that other muscarinic receptor subtypes might have been responsible for the neuroprotective effects that had previously been attributed to the M$_1$ receptor. Hence, in the present study, we examined the potential role of all five muscarinic receptor subtypes on neuroprotection in the RGC layer. Importantly, the animals used in this study were N10 congenic, which
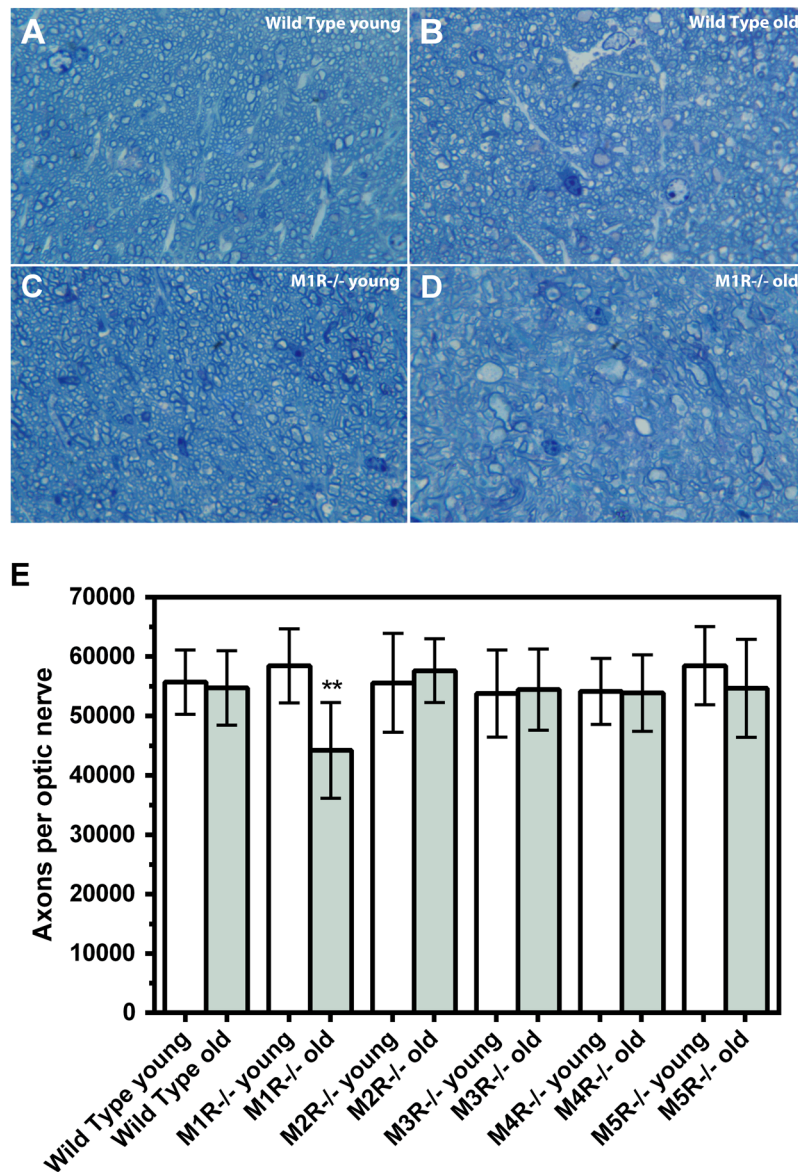
Axons in Optic Nerve Cross-Sections

Figure 4. Example of photographs taken from optic nerve cross-sections of wild-type and M1R−/− mice. at both age categories (**A–D**; scale bars 10 µm). The number of optic nerve axons was lower in old M1R−/− mice compared to younger mice of the same genetic background (D, **p < 0.01).

makes it much less likely that strain differences may have affected neuron survival. We additionally examined animals at advanced age, which is a crucial risk factor for glaucoma.

Of note, M1R−/− mice had significantly fewer neurons in the RGC layer and axons in the optic nerve at the age of 15 months compared to the age of 5 months. All other genotypes including wild-type mice had similar neuron numbers at young and old age. In previous studies that examined RGCs in mice at different ages also no signs of RGC loss were found in wild-type mice of the C57BL/6 background until the age of 14 months[32] or even 16 to 23 months[33].

The neuron loss in M1R−/− mice is unlikely to be caused by an increased IOP, the major risk factor for glaucoma, because no differences in IOP were found between young and aged M1R−/− mice as well as between individual mouse genotypes. Although activation of muscarinic receptors by agonists, such as pilocarpine or carbachol was shown to reduce IOP in humans and mice[34–36], it does not necessarily mean that the lack or blockade of muscarinic receptors evokes an opposite effect, at least in eyes without preexisting anterior eye abnormalities. For example, no marked impact on IOP has been shown for the muscarinic receptor antagonist, atropine, when applied in humans on a long-term basis[37,38]. Hence, it is possible that muscarinic receptors only affect the IOP level when activated.

Prooxidative Redox Genes

Antioxidative Redox Genes
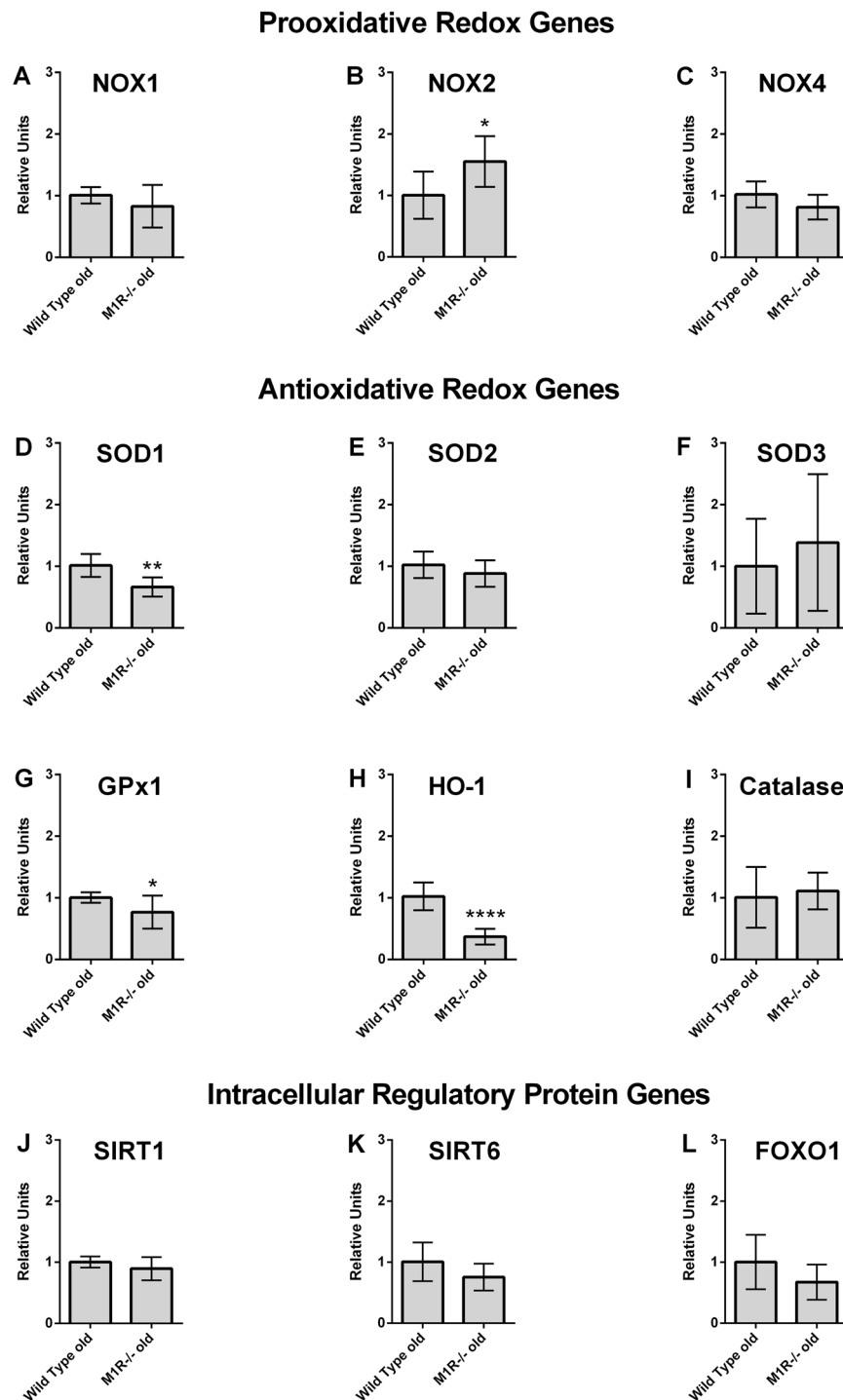
Intracellular Regulatory Protein Genes

Figure 5. Messenger RNA expression of prooxidative genes (NOX1, NOX2, NOX4), antioxidative genes (SOD1, SOD2, SOD3, GPx1, HO-1, Catalase) and of genes coding for intracellular regulatory proteins involved in aging (SIRT1, SIRT6, FOXO1) in aged wild-type and M1R−/− mice. Expression of NOX2 was significantly increased in aged M1R−/− mice. In contrast, the antioxidative redox genes, SOD1, GPx1 and HO-1, showed reduced expression levels in aged M1R−/− mice. Data are presented as mean ± SD (n = 8 per genotype; *p < 0.05; **p < 0.01; ****p < 0.0001).

The present study supports previous reports suggesting that muscarinic receptor agonists exert neuroprotective effects in the eye not only via IOP reduction, but also by direct action on retinal neurons[27,39]. In the retina, cholinergic amacrine cells are the source of the physiological muscarinic receptor agonist, acetylcholine, which was shown to transmit cholinergic signals to RGCs via muscarinic and nicotinic receptors[40–43]. However, although multiple muscarinic receptor subtypes, including the M_1 receptor, were detected on RGCs, amacrine cells and bipolar cells, the specific role of the individual subtypes in retinal cell-to-cell signaling is still poorly understood[31,42]. Overlapping
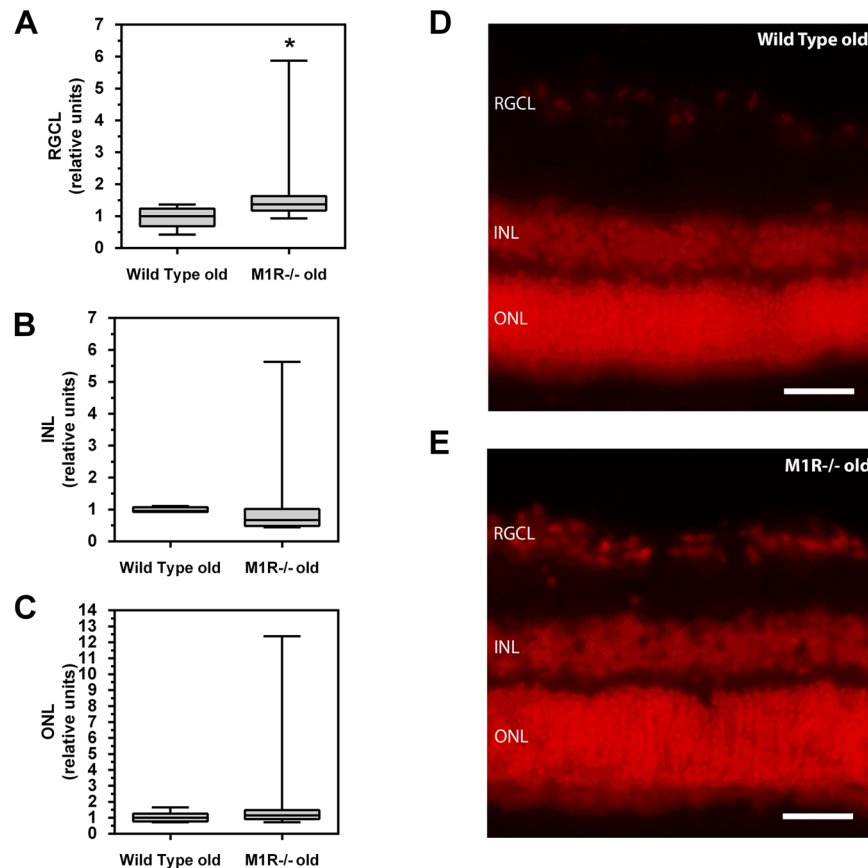
DHE Staining Intensity

Figure 6. DHE staining intensity in the retinal ganglion cell layer (RGCL, **A**), the inner nuclear layer (INL, **B**) and the outer nuclear layer (ONL, **C**) in aged wild-type and M1R−/− mice. DHE staining intensity was markedly elevated in the RGCL of aged M1R−/− mice (*$P < 0.05$) suggesting higher ROS levels. Pictures of DHE-stained retinal cryosections for aged wild-type (**D**; scale bar 50 μm) and M1R−/− mice (**E**; scale bar 50 μm).

receptor subtype expression patterns in individual cell types, limited selectivity of pharmacological ligands and low specificity of antibodies for individual muscarinic receptor subtypes are obstacles in this regard[28,44,45]. Genetically modified animals lacking individual muscarinic receptor subtypes may be useful to circumvent these problems.

In the present study, we assessed neuron loss using two approaches. In the retina, we counted cells in the RGC layer based on morphological criteria of cell nuclei stained with cresyl blue. The staining method has the advantage of being fast and inexpensive, yielding simultaneous information on multiple cell types, being independent on axonal transport properties compared to retrograde labeling techniques, and of circumventing problems of antibody specificity to retinal cells[46–48]. However, this method has also some weaknesses. First, it does not allow to clearly distinguish between RGCs and other neurons, like displaced amacrine cells, because of some overlap in nuclear size and shape[49,50]. Second, the counting method has not been fully validated and, thus, the calculated cell number may vary depending on the evaluator. Third, it should be considered that the presented mathematical average of the sampled areas multiplied by retinal area may result in calculated cell numbers that are skewed from the actual number, because cell density in the RGC layer markedly differs between the center and the periphery of the retina[49].

In order to specify the number of RGCs, we additionally calculated axons of RGCs in optic nerve cross sections. The axon number as a percentage of neurons in the RGC layer was between 51,6% and 56,6% among all our mouse groups, which is similar to other studies in mice and can be explained by the fact that only around half of the neurons in the RGC layer are actually RGCs[51]. Remarkably, the axon number was markedly reduced in aged M1R−/− mice supporting the notion that RGC survival is compromised with aging when the M_1 receptor is lacking. However, the relation of axons in optic nerve cross sections to neurons in the RGC layer did not change with age in any of the mouse genotypes, including M1R−/− mice, suggesting that neuron loss in the RGC layer observed in M1R−/− was not selectively affecting RGCs.

Muscarinic receptor-independent gene mutations of the knockout mice that may affect neuron survival in the retina should also be considered. Notably, C57BL/6N substrains were shown to harbor the recessive single base pair mutation, rd8, in the Crb1 gene, which causes retinal degeneration 8, a mild form of retinal degeneration characterized by focal external limiting membrane and photoreceptor defects[52,53]. The onset of the phenotype appears to be between 2 and 6 weeks of age[54]. As opposed to any of the five muscarinic receptor subtype genes,

9

the rd8 mutation is located on chromosome 1, and is not linked with any of the muscarinic receptor mutations. Moreover, rd8 mutation has not been associated with neuron loss in the RGC layer. Thus, it is very unlikely that this mutation is responsible for the neuron loss that we observed in aged M1R−/− mice.

The age-dependent neuron loss in the retina and optic nerve of M1R−/− mice seems highly relevant regarding the pathophysiology of normal tension glaucoma. Most known mouse models of normal tension glaucoma, like excitatory amino-acid carrier 1 (EAAC1), glutamate/aspartate transporter (GLAST) and superoxide dismutase 1 (SOD1) knockout mice are actually models of increased oxidative stress[55–57]. Remarkably, we found that mRNA expression of the prooxidative NOX2 was increased in aged M1R−/− mice. Previous studies reported an increased NOX2 expression to be involved in the pathophysiology of various retinal diseases. For example, NOX2-generated ROS were shown to contribute to retinal vascular injury and to acceleration of vascular endothelial cell senescence in diabetic mouse retinas[58,59]. Moreover, a correlation between elevated retinal apoptotic markers and increased NOX2 expression has been reported in diabetic mice[60]. Also, glucotoxic and lipotoxic insults were shown to promote ROS production in retinal vascular endothelial cells via activation of NOX2[61]. In a mouse model of oxygen-induced retinopathy, NOX2-generated ROS facilitated neovascularization[62]. NOX2 was also shown to promote apoptosis in the retina after ischemic injury[63]. Moreover, NOX2 activity was suggested to play a primary role in acute and chronic conditions associated with retinal vascular inflammatory reactions[64]. In addition to an increased NOX2 expression, we found that mRNA levels of the antioxidative enzymes, SOD1, HO-1 and GPx1, were reduced in aged M1R−/− mice. Importantly, each of the three enzymes has previously been reported to play a neuroprotective role in the retina. For example, the lack of SOD1 resulted in an increased functional impairment of retinal neurons following exposure to paraquat and hyperoxia[65]. Moreover, the lack of SOD1 caused neurodegeneration in the retina of respective KO mice[66]. The lack of SOD1 is correlated with an accelerated aging phenotype. Conversely, an overexpression of SOD1 has been found protective against changes seen in diabetic retinopathy[67]. Our findings are also in line with a study reporting that 24-week-old SOD1 KO mice showed morphological alterations similar to those observed in normal tension glaucoma[57]. In the same study, SOD1 serum levels were found to be reduced in patients with normal tension glaucoma compared to healthy controls[57]. Apart from SOD1, also HO-1 and GPx1 have been proposed to play a protective role against ocular diseases like diabetic and light-induced retinopathies[68,69]. With regard to neuronal degeneration, it has been demonstrated that lower levels of HO-1 increased susceptibility of RGCs to apoptosis[70]. Moreover, reduced levels or the complete lack of GPx1 were shown to enhance the functional, cellular and vascular damage in the retina induced by light[71], hypoxia[72] and retinopathy of prematurity[73].

Taken together, our results suggest that in addition to increased NOX2 mRNA expression levels, aged M1R−/− mice have also a reduced antioxidative capacity in the retina due to downregulation of various antioxidative enzymes, such as SOD1, HO-1 and GPx1, whose lack has been linked to retinal neuron damage. The increased ROS levels that we found in the RGC layer of aged M1R−/− mice support our mRNA expression data. Our findings provide the first direct evidence that the lack of the M_1 receptor leads to accelerated RGC loss in mice via an increase of oxidative stress in the retina. From a clinical point of view, M_1 receptor agonists may become useful to treat neurodegenerative ocular diseases, such as glaucoma. Moreover, it would be important to investigate whether certain polymorphisms of the M_1 receptor gene are associated with glaucoma development in humans.

Data Availability
Data are available after request to the author.

References

1. Quigley, H. A. & Broman, A. T. The number of people with glaucoma worldwide in 2010 and 2020. *Br J Ophthalmol* **90**, 262–267, 90/3/262 https://doi.org/10.1136/bjo.2005.081224 (2006).
2. Tham, Y. C. *et al.* Global prevalence of glaucoma and projections of glaucoma burden through 2040: a systematic review and meta-analysis. *Ophthalmology* **121**, 2081–2090, https://doi.org/10.1016/j.ophtha.2014.05.013 (2014).
3. Yoshida, M., Kunimatsu-Sanuki, S., Omodaka, K. & Nakazawa, T. Structure/function relationship between wide-scan binocular OCT images and the integrated visual field in glaucoma patients. *Clinical & experimental ophthalmology* **44**, 526–528, https://doi.org/10.1111/ceo.12701 (2016).
4. Shukla, M., Boontem, P., Reiter, R. J., Satayavivad, J. & Govitrapong, P. Mechanisms of Melatonin in Alleviating Alzheimer's Disease. *Current neuropharmacology*, https://doi.org/10.2174/1570159X15666170313123454 (2017).
5. Gupta, V. *et al.* BDNF impairment is associated with age-related changes in the inner retina and exacerbates experimental glaucoma. *Biochimica et biophysica acta* **1842**, 1567–1578, https://doi.org/10.1016/j.bbadis.2014.05.026 (2014).
6. Ferreira-Vieira, T. H., Guimaraes, I. M., Silva, F. R. & Ribeiro, F. M. Alzheimer's disease: Targeting the Cholinergic System. *Current neuropharmacology* **14**, 101–115 (2016).
7. Wu, W. Y. *et al.* Novel multitarget-directed tacrine derivatives as potential candidates for the treatment of Alzheimer's disease. *Journal of enzyme inhibition and medicinal chemistry* **32**, 572–587, https://doi.org/10.1080/14756366.2016.1210139 (2017).
8. Pienaar, I. S. *et al.* Pharmacogenetic stimulation of cholinergic pedunculopontine neurons reverses motor deficits in a rat model of Parkinson's disease. *Molecular neurodegeneration* **10**, 47, https://doi.org/10.1186/s13024-015-0044-5 (2015).
9. Marvanova, M. & Henkel, P. J. Community Pharmacists' Knowledge Regarding Donepezil Averse Effects and Self-Care Recommendations for Insomnia for Persons with AD. *Pharmacy* **5**, https://doi.org/10.3390/pharmacy5030042 (2017).
10. Nathan, P. J. *et al.* The potent M1 receptor allosteric agonist GSK1034702 improves episodic memory in humans in the nicotine abstinence model of cognitive dysfunction. *The international journal of neuropsychopharmacology* **16**, 721–731, https://doi.org/10.1017/S1461145712000752 (2013).
11. Chintamaneni, P. K., Krishnamurthy, P. T., Rao, P. V. & Pindiprolu, S. S. Surface modified nano-lipid drug conjugates of positive allosteric modulators of M1 muscarinic acetylcholine receptor for the treatment of Alzheimer's disease. *Medical hypotheses* **101**, 17–22, https://doi.org/10.1016/j.mehy.2017.01.026 (2017).
12. Bradley, S. J. *et al.* M1 muscarinic allosteric modulators slow prion neurodegeneration and restore memory loss. *The Journal of clinical investigation* **127**, 487–499, https://doi.org/10.1172/JCI87526 (2017).
13. Duncan, G. & Collison, D. J. Role of the non-neuronal cholinergic system in the eye: a review. *Life Sci* **72**, 2013–2019, doi:S002432050300064X (2003).
14. Gericke, A. *et al.* Identification of the muscarinic acetylcholine receptor subtype mediating cholinergic vasodilation in murine retinal arterioles. *Invest Ophthalmol Vis Sci* **52**, 7479–7484, iovs.11-7370 https://doi.org/10.1167/iovs.11-7370.

15. Almasieh, M. *et al*. Acetylcholinesterase inhibition promotes retinal vasoprotection and increases ocular blood flow in experimental glaucoma. *Invest Ophthalmol Vis Sci* **54**, 3171–3183, https://doi.org/10.1167/iovs.12-11481 (2013).
16. Ikarashi, R. *et al*. Regulation of molecular clock oscillations and phagocytic activity via muscarinic Ca2+ signaling in human retinal pigment epithelial cells. *Scientific reports* **7**, 44175, https://doi.org/10.1038/srep44175 (2017).
17. Fisahn, A. *et al*. Muscarinic induction of hippocampal gamma oscillations requires coupling of the M1 receptor to two mixed cation currents. *Neuron* **33**, 615–624 (2002).
18. Gomeza, J. *et al*. Pronounced pharmacologic deficits in M2 muscarinic acetylcholine receptor knockout mice. *Proceedings of the National Academy of Sciences of the United States of America* **96**, 1692–1697 (1999).
19. Gomeza, J. *et al*. Enhancement of D1 dopamine receptor-mediated locomotor stimulation in M(4) muscarinic acetylcholine receptor knockout mice. *Proceedings of the National Academy of Sciences of the United States of America* **96**, 10483–10488 (1999).
20. Yamada, M. *et al*. Cholinergic dilation of cerebral blood vessels is abolished in M(5) muscarinic acetylcholine receptor knockout mice. *Proceedings of the National Academy of Sciences of the United States of America* **98**, 14096–14101, https://doi.org/10.1073/pnas.251542998 (2001).
21. Yamada, M. *et al*. Mice lacking the M3 muscarinic acetylcholine receptor are hypophagic and lean. *Nature* **410**, 207–212, https://doi.org/10.1038/35065604 (2001).
22. Laspas, P. *et al*. Autoreactive antibodies and loss of retinal ganglion cells in rats induced by immunization with ocular antigens. *Invest Ophthalmol Vis Sci* **52**, 8835–8848, https://doi.org/10.1167/iovs.10-6889 (2011).
23. Xia, N. *et al*. Uncoupling of Endothelial Nitric Oxide Synthase in Perivascular Adipose Tissue of Diet-Induced Obese Mice. *Arteriosclerosis, thrombosis, and vascular biology* **36**, 78–85, https://doi.org/10.1161/ATVBAHA.115.306263 (2016).
24. Li, H. *et al*. Reversal of endothelial nitric oxide synthase uncoupling and up-regulation of endothelial nitric oxide synthase expression lowers blood pressure in hypertensive rats. *Journal of the American College of Cardiology* **47**, 2536–2544, https://doi.org/10.1016/j.jacc.2006.01.071 (2006).
25. Pereira, S. P., Medina, S. V. & Araujo, E. G. Cholinergic activity modulates the survival of retinal ganglion cells in culture: the role of M1 muscarinic receptors. *Int J Dev Neurosci* **19**, 559–567, S0736574801000430 (2001).
26. Zhou, W. *et al*. Neuroprotection of muscarinic receptor agonist pilocarpine against glutamate-induced apoptosis in retinal neurons. *Cellular and molecular neurobiology* **28**, 263–275, https://doi.org/10.1007/s10571-007-9251-0 (2008).
27. Almasieh, M., Zhou, Y., Kelly, M. E., Casanova, C. & Di Polo, A. Structural and functional neuroprotection in glaucoma: role of galantamine-mediated activation of muscarinic acetylcholine receptors. *Cell Death Dis* **1**, e27, https://doi.org/10.1038/cddis.2009.23 (2010).
28. Caulfield, M. P. & Birdsall, N. J. International Union of Pharmacology. XVII. Classification of muscarinic acetylcholine receptors. *Pharmacol Rev* **50**, 279–290 (1998).
29. Giachetti, A., Giraldo, E., Ladinsky, H. & Montagna, E. Binding and functional profiles of the selective M1 muscarinic receptor antagonists trihexyphenidyl and dicyclomine. *Br J Pharmacol* **89**, 83–90 (1986).
30. Ukena, D., Wehinger, C., Engelstatter, R., Steinijans, V. & Sybrecht, G. W. The muscarinic M1-receptor-selective antagonist, telenzepine, had no bronchodilatory effects in COPD patients. *The European respiratory journal* **6**, 378–382 (1993).
31. Laspas, P. *et al*. Effect of the M1 Muscarinic Acetylcholine Receptor on Retinal Neuron Number Studied with Gene-Targeted Mice. *Journal of molecular neuroscience: MN* **56**, 472–479, https://doi.org/10.1007/s12031-015-0524-7 (2015).
32. Kimball, E. C. *et al*. The effects of age on mitochondria, axonal transport, and axonal degeneration after chronic IOP elevation using a murine ocular explant model. *Exp Eye Res* **172**, 78–85, https://doi.org/10.1016/j.exer.2018.04.001 (2018).
33. Kashiwagi, K., Ito, S., Maeda, S. & Kato, G. A Ser75-to-Asp phospho-mimicking mutation in Src accelerates ageing-related loss of retinal ganglion cells in mice. *Scientific reports* **7**, 16779, https://doi.org/10.1038/s41598-017-16872-7 (2017).
34. Akaishi, T., Odani-Kawabata, N., Ishida, N. & Nakamura, M. Ocular hypotensive effects of anti-glaucoma agents in mice. *Journal of ocular pharmacology and therapeutics: the official journal of the Association for Ocular Pharmacology and Therapeutics* **25**, 401–408, https://doi.org/10.1089/jop.2009.0006 (2009).
35. Avila, M. Y., Carre, D. A., Stone, R. A. & Civan, M. M. Reliable measurement of mouse intraocular pressure by a servo-null micropipette system. *Invest Ophthalmol Vis Sci* **42**, 1841–1846 (2001).
36. Fry, L. L. Comparison of the postoperative intraocular pressure with Betagan, Betoptic, Timoptic, Iopidine, Diamox, Pilopine Gel, and Miostat. *Journal of cataract and refractive surgery* **18**, 14–19 (1992).
37. Lee, C. Y., Sun, C. C., Lin, Y. F. & Lin, K. K. Effects of topical atropine on intraocular pressure and myopia progression: a prospective comparative study. *BMC ophthalmology* **16**, 114, https://doi.org/10.1186/s12886-016-0297-y (2016).
38. Wu, T. E., Yang, C. C. & Chen, H. S. Does atropine use increase intraocular pressure in myopic children? *Optom Vis Sci* **89**, E161–167, https://doi.org/10.1097/OPX.0b013e31823ac4c1 (2012).
39. Tan, P. P. *et al*. Activation of muscarinic receptors protects against retinal neurons damage and optic nerve degeneration *in vitro* and *in vivo* models. *CNS neuroscience & therapeutics* **20**, 227–236, https://doi.org/10.1111/cns.12187 (2014).
40. Baldridge, W. H. Optical recordings of the effects of cholinergic ligands on neurons in the ganglion cell layer of mammalian retina. *The Journal of neuroscience: the official journal of the Society for Neuroscience* **16**, 5060–5072 (1996).
41. O'Malley, D. M., Sandell, J. H. & Masland, R. H. Co-release of acetylcholine and GABA by the starburst amacrine cells. *The Journal of neuroscience: the official journal of the Society for Neuroscience* **12**, 1394–1408 (1992).
42. Strang, C. E., Long, Y., Gavrikov, K. E., Amthor, F. R. & Keyser, K. T. Nicotinic and muscarinic acetylcholine receptors shape ganglion cell response properties. *Journal of neurophysiology* **113**, 203–217, https://doi.org/10.1152/jn.00405.2014 (2015).
43. Yamada, E. S. *et al*. Synaptic connections of starburst amacrine cells and localization of acetylcholine receptors in primate retinas. *The Journal of comparative neurology* **461**, 76–90, https://doi.org/10.1002/cne.10672 (2003).
44. Pradidarcheep, W., Labruyere, W. T., Dabhoiwala, N. F. & Lamers, W. H. Lack of specificity of commercially available antisera: better specifications needed. *The journal of histochemistry and cytochemistry: official journal of the Histochemistry. Society* **56**, 1099–1111, https://doi.org/10.1369/jhc.2008.952101 (2008).
45. Wess, J. Molecular biology of muscarinic acetylcholine receptors. *Critical reviews in neurobiology* **10**, 69–99 (1996).
46. Baker, M. Reproducibility crisis: Blame it on the antibodies. *Nature* **521**, 274–276, https://doi.org/10.1038/521274a (2015).
47. Kobbert, C. *et al*. Current concepts in neuroanatomical tracing. *Progress in neurobiology* **62**, 327–351 (2000).
48. Soto, I. *et al*. Retinal ganglion cells downregulate gene expression and lose their axons within the optic nerve head in a mouse glaucoma model. *The Journal of neuroscience: the official journal of the Society for Neuroscience* **28**, 548–561, https://doi.org/10.1523/JNEUROSCI.3714-07.2008 (2008).
49. Drager, U. C. & Olsen, J. F. Ganglion cell distribution in the retina of the mouse. *Invest Ophthalmol Vis Sci* **20**, 285–293 (1981).
50. Hedberg-Buenz, A. *et al*. Quantitative measurement of retinal ganglion cell populations via histology-based random forest classification. *Exp Eye Res* **146**, 370–385, https://doi.org/10.1016/j.exer.2015.09.011 (2016).
51. Schlamp, C. L. *et al*. Evaluation of the percentage of ganglion cells in the ganglion cell layer of the rodent retina. *Mol Vis* **19**, 1387–1396 (2013).
52. Mehalow, A. K. *et al*. CRB1 is essential for external limiting membrane integrity and photoreceptor morphogenesis in the mammalian retina. *Human molecular genetics* **12**, 2179–2189, https://doi.org/10.1093/hmg/ddg232 (2003).
53. Mattapallil, M. J. *et al*. The Rd8 mutation of the Crb1 gene is present in vendor lines of C57BL/6N mice and embryonic stem cells, and confounds ocular induced mutant phenotypes. *Invest Ophthalmol Vis Sci* **53**, 2921–2927, https://doi.org/10.1167/iovs.12-9662 (2012).

54. Pritchett-Corning, K. R., Clifford, C. B., Elder, B. J. & Vezina, M. Retinal lesions and other potential confounders of ocular research in inbred mice. *Invest Ophthalmol Vis Sci* **53**, 3764–3765, https://doi.org/10.1167/iovs.12-10056 (2012).
55. Akaiwa, K. *et al.* Topical Ripasudil Suppresses Retinal Ganglion Cell Death in a Mouse Model of Normal Tension Glaucoma. *Invest Ophthalmol Vis Sci* **59**, 2080–2089, https://doi.org/10.1167/iovs.17-23276 (2018).
56. Sano, H. *et al.* Differential effects of N-acetylcysteine on retinal degeneration in two mouse models of normal tension glaucoma. *Cell Death Dis* **10**, 75, https://doi.org/10.1038/s41419-019-1365-z (2019).
57. Yuki, K. *et al.* Retinal ganglion cell loss in superoxide dismutase 1 deficiency. *Invest Ophthalmol Vis Sci* **52**, 4143–4150, https://doi.org/10.1167/iovs.10-6294 (2011).
58. Rojas, M. *et al.* NOX2-Induced Activation of Arginase and Diabetes-Induced Retinal Endothelial Cell Senescence. *Antioxidants* **6**, https://doi.org/10.3390/antiox6020043 (2017).
59. Rojas, M. *et al.* Requirement of NOX2 expression in both retina and bone marrow for diabetes-induced retinal vascular injury. *PloS one* **8**, e84357, https://doi.org/10.1371/journal.pone.0084357 (2013).
60. Mohammad, G. *et al.* Mutual enhancement between high-mobility group box-1 and NADPH oxidase-derived reactive oxygen species mediates diabetes-induced upregulation of retinal apoptotic markers. *Journal of physiology and biochemistry* **71**, 359–372, https://doi.org/10.1007/s13105-015-0416-x (2015).
61. Kumar, B., Kowluru, A. & Kowluru, R. A. Lipotoxicity augments glucotoxicity-induced mitochondrial damage in the development of diabetic retinopathy. *Invest Ophthalmol Vis Sci* **56**, 2985–2992, https://doi.org/10.1167/iovs.15-16466 (2015).
62. Chan, E. C. *et al.* Involvement of Nox2 NADPH oxidase in retinal neovascularization. *Invest Ophthalmol Vis Sci* **54**, 7061–7067, https://doi.org/10.1167/iovs.13-12883 (2013).
63. Yokota, H. *et al.* Neuroprotection from retinal ischemia/reperfusion injury by NOX2 NADPH oxidase deletion. *Invest Ophthalmol Vis Sci* **52**, 8123–8131, https://doi.org/10.1167/iovs.11-8318 (2011).
64. Al-Shabrawey, M. *et al.* Role of NADPH oxidase in retinal vascular inflammation. *Invest Ophthalmol Vis Sci* **49**, 3239–3244, https://doi.org/10.1167/iovs.08-1755 (2008).
65. Dong, A. *et al.* Superoxide dismutase 1 protects retinal cells from oxidative damage. *Journal of cellular physiology* **208**, 516–526, https://doi.org/10.1002/jcp.20683 (2006).
66. Hashizume, K. *et al.* Retinal dysfunction and progressive retinal cell death in SOD1-deficient mice. *The American journal of pathology* **172**, 1325–1331, https://doi.org/10.2353/ajpath.2008.070730 (2008).
67. Berkowitz, B. A., Gradianu, M., Bissig, D., Kern, T. S. & Roberts, R. Retinal ion regulation in a mouse model of diabetic retinopathy: natural history and the effect of Cu/Zn superoxide dismutase overexpression. *Invest Ophthalmol Vis Sci* **50**, 2351–2358, https://doi.org/10.1167/iovs.08-2918 (2009).
68. Shanab, A. Y. *et al.* Candesartan stimulates reparative angiogenesis in ischemic retinopathy model: role of hemeoxygenase-1 (HO-1). *Angiogenesis* **18**, 137–150, https://doi.org/10.1007/s10456-014-9451-4 (2015).
69. Pilat, A., Herrnreiter, A. M., Skumatz, C. M., Sarna, T. & Burke, J. M. Oxidative stress increases HO-1 expression in ARPE-19 cells, but melanosomes suppress the increase when light is the stressor. *Invest Ophthalmol Vis Sci* **54**, 47–56, https://doi.org/10.1167/iovs.12-11153 (2013).
70. Fan, J., Xu, G., Jiang, T. & Qin, Y. Pharmacologic induction of heme oxygenase-1 plays a protective role in diabetic retinopathy in rats. *Invest Ophthalmol Vis Sci* **53**, 6541–6556, https://doi.org/10.1167/iovs.11-9241 (2012).
71. Gosbell, A. D. *et al.* Retinal light damage: structural and functional effects of the antioxidant glutathione peroxidase-1. *Invest Ophthalmol Vis Sci* **47**, 2613–2622, https://doi.org/10.1167/iovs.05-0962 (2006).
72. Tan, S. M. *et al.* Ebselen by modulating oxidative stress improves hypoxia-induced macroglial Muller cell and vascular injury in the retina. *Exp Eye Res* **136**, 1–8, https://doi.org/10.1016/j.exer.2015.04.015 (2015).
73. Tan, S. M., Stefanovic, N., Tan, G., Wilkinson-Berka, J. L. & de Haan, J. B. Lack of the antioxidant glutathione peroxidase-1 (GPx1) exacerbates retinopathy of prematurity in mice. *Invest Ophthalmol Vis Sci* **54**, 555–562, https://doi.org/10.1167/iovs.12-10685 (2013).

Acknowledgements

Author Contributions

P. Laspas performed the animal examinations, collection of tissue, histological examinations and wrote the manuscript; M.B. Zhutdieva and A. Musayeva counted cells and axons; J. Kouchek Zadeh performed and analyzed the DHE staining; C. Brochhausen performed histological examinations and provided essential materials; J. Wess provided the mice; N. Xia and H. Li performed and analyzed the PCR; N. Pfeiffer provided essential materials; A. Gericke designed the study, provided essential materials, and analyzed data. All authors read and revised the manuscript.

Additional Information

Competing Interests: The authors declare no competing interests.

Publisher's note: Springer Nature remains neutral with regard to jurisdictional claims in published maps and institutional affiliations.